

Title	Self-organized metallic islands on nano-patterned silicon substrate
Author(s)	Agnus, G.; Maroutian, T.; Fleurence, A.; Bartenlian, B.; Hanbucken, M.; Beauvillain, P.
Citation	Applied Physics Letters, 103(12): 123117-1-123117-4
Issue Date	2013-09-20
Type	Journal Article
Text version	publisher
URL	http://hdl.handle.net/10119/12987
Rights	Copyright 2013 American Institute of Physics. This article may be downloaded for personal use only. Any other use requires prior permission of the author and the American Institute of Physics. The following article appeared in G. Agnus, T. Maroutian, A. Fleurence, B. Bartenlian, M. Hanbucken, P. Beauvillain , Applied Physics Letters, 103(12), 123117 (2013) and may be found at
Description	



Self-organized metallic islands on nano-patterned silicon substrate

G. Agnus,^{1,a)} T. Maroutian,¹ A. Fleurence,^{2,b)} B. Bartenlian,¹ M. Hanbücken,³ and P. Beauvillain¹

¹*Institut d'Electronique Fondamentale, Univ. Paris-Sud, CNRS UMR 8622, Orsay, France*

²*School of Material Science, Japan Advanced Institute of Science Technology, 1-1 Asahidai Ishikawa 923-1292, Japan*

³*Aix Marseille Univ, CNRS UMR 7325, CINaM, F-13288 Marseille, France*

(Received 26 July 2013; accepted 3 September 2013; published online 20 September 2013)

Combining the self-organized growth of nanometer size islands with the use of a pre-patterned substrate, the fabrication of a metallic nanoparticle array with sub-100 nm period is demonstrated. The array pattern is artificially defined through conventional lithography on a Si substrate. Two passivation steps are used first *ex situ* with a wet hydrogenation followed by the *in situ* formation under ultrahigh vacuum of an Au-Si wetting layer. This allows for the subsequent nucleation and growth of Au on an atomically clean surface. The long range order of the nanoparticle array is preserved over the whole millimeter-size patterned area. © 2013 AIP Publishing LLC. [<http://dx.doi.org/10.1063/1.4821646>]

Metallic nanoparticles exhibit unique electronic, magnetic, photonic, and catalytic properties which are exploited in application fields such as energy, photonics, or sensing.^{1–3} In particular, gold nanoislands are extensively used, for example, to immobilize DNA chains in biosensors,⁴ to catalyze the growth of unidimensional objects such as nanowires⁵ or carbon nanotubes,⁶ or to fabricate magnetic nanodots.^{7,8} The organization and positioning of nanoparticles on semiconductor substrates is a great challenge in order to take advantage of their properties and fabricate innovative integrated devices;^{9–11} a main concern being to address nanometer size objects. While self-organization on naturally occurring patterns^{12,13} or through chemical interactions¹⁴ has the advantage of easy production of nano-objects with high crystalline quality and ultra-high density on large scale surfaces, the array parameters (pattern shape, periodicity) are generally imposed by the particular material/substrate system considered. Additionally, due to nearest-neighbor or strain-based interactions between particles their correlated ordering extends from nanometer to micrometer range but cannot be expected to hold up to millimeter sizes. On the other hand, direct patterning techniques which allow for arbitrary pattern designs down to the nanometer scale like with e-beam¹⁵ or nanoimprint¹⁶ lithographies can be limited in terms of patterned area, particle edge roughness, and crystalline quality.

A hybrid method was proposed by Ogino and co-workers,¹⁷ in which the substrate is artificially patterned in order to combine the advantages of high quality self-organized nano-objects to the full control of the array geometry with long range order. This approach was successfully applied to organize gold islands on silicon with micrometer-size patterns,¹⁷ and reproduced for Ge/Si system down to a few hundred nanometers scale.^{18,19} In this work, we demonstrate the extension of this approach down to the sub-100 nm scale in the case

of metallic nanoparticles, while preserving long range order on the whole patterned area.

The method relies on the elaboration of a patterned Si substrate at the nanometer scale through conventional lithography and reactive ion etching with an atomically clean surface compatible with the self-organized growth of metallic islands in an ultrahigh vacuum (UHV) chamber. This is made possible through the use of a passivating step allowing for the diffusion and nucleation of species as on state-of-the-art UHV prepared surfaces. While the array parameters are designed during a so-called “top-down” approach, the actual elaboration of the nanostructures themselves does not require further processing thus keeping the intrinsic advantages of self-organized objects. Our elaboration scheme unfolds as follows: (i) artificially defined regular array of nucleation sites, (ii) transfer of this array into an UHV deposition chamber, and (iii) self-organized island nucleation and growth with suitable parameters to obtain the desired positioning of nanometer size islands. The array has been chosen as a hole pattern on silicon, with gold islands as metallic nanoparticles.

Si(111) substrates are patterned using a step of e-beam lithography followed by reactive ion etching (RIE). A 40 nm-thick layer of poly-methyl-metha-acrylate (PMMA) is first spin-coated on the sample followed by a 1 h annealing at 175 °C. E-beam lithography is then performed to create an array of 30 nm diameter apertures in the resist with a periodicity of 80 nm. This periodicity was chosen similar to the unidimensional array of step bunches used for the self-organization of Au-Si islands in our previous work.^{8,20} A patterned area in the mm² range was made during a single step of e-beam lithography. Alternative lithographic techniques such as nanoimprint²¹ are under development for the large scale and low cost sample fabrication. The resist pattern is then transferred in silicon during a step of RIE followed by resist striping. At this stage, the surface is comprised of oxidized silicon patterned with 30 nm-diameter circles, aspect ratio close to one and a periodicity of 80 nm.

Aiming at the self-organization of gold islands on this pre-patterned substrate, the surface cleanliness is a key

^{a)}Electronic mail: guillaume.agnus@u-psud.fr

^{b)}This research was performed while A. Fleurence was at Institut d'Electronique Fondamentale, Univ. Paris- Sud, CNRS UMR 8622, Orsay, France

parameter which will notably govern the final island population. In particular, silicon oxidation, the presence of resist residues or any other defect can form nucleation sites that will influence the island positions. We thus performed a drastic cleaning procedure using several steps of oxidation with acids followed by oxide removal using fluorhydric acid to remove all these surface defects. Before introduction under UHV, a final deoxidation is performed followed by a step of passivation using ammonium fluoride to prevent further oxidation.²²

Fig. 1 presents scanning tunneling microscopy (STM) images taken under UHV of the Si(111) surface after cleaning and hydrogenation. STM image of Fig. 1(a), taken out of the patterned area, shows a very clean surface with visible atomic steps demonstrating the surface quality after such wet preparation. Such images are similar to state of the art silicon passivation using NH_4F seen in the literature.²³ However, the use of such wet preparation gave rise to inhomogeneities of the surface atomic termination between samples. In order to smooth these variations, we performed a first 0.5 monolayer (ML) gold deposition followed by 15 min annealing at 600 °C in order to form a $\sqrt{3} \times \sqrt{3}$ -reconstructed Au-Si wetting layer.²⁰ This procedure was used prior to all the growths from which the results shown in this work are extracted. Images taken in the patterned area (Fig. 1(b)) after the aforementioned preparation exhibit a 80 nm square-array of triangles, corresponding to the e-beam lithography design shown as an inset on the same figure (scanning electron microscopy—SEM). While holes were circular after lithography and etching, the triangular shape appears after the final $\text{NH}_4\text{F}/\text{HF}$ dipping and is linked to the preferential etching of the (111) planes with ammonium fluoride.²⁴ To avoid coalescence between holes at this stage, the square pattern is designed along the [1–10] and [11–2] directions. On the STM image, steps are also visible and their density is much higher in the holes to accommodate the local higher miscut angle. We aim at taking benefit of this bi-dimensional arrangement of steps to guide the growth of the metallic islands.

We performed gold depositions on patterned Si(111) substrates with varying growth parameters such as temperature and thickness in order to optimize the organization of the islands on the predefined pattern. All temperatures were above 340 °C so that, as shown in our previous work,^{8,20} the surface is comprised of hemispherical Au silicide islands on the $\sqrt{3} \times \sqrt{3}$ -reconstructed Au-Si layer. While islands are observed by STM in between the holes at the lowest investigated temperatures, they disappear when the temperature is increased up to around 415 °C as will be discussed later. In Fig. 2, typical images of self-organized Au-Si islands on the hole array are displayed, taken after 4 ML Au growth at 415 °C. All Au-Si islands are located in the holes and the filling percentage is larger than 90%. The mean island size is around 20 nm and the 80 nm periodicity corresponds to a density of 1.56×10^{10} islands/cm². In agreement with previous studies of Au island nucleation on stepped Si surfaces,^{17,25} the Au silicide islands are wetting preferentially the high curvature regions where step density is the highest and thus exchange of atoms with the Si substrate the easiest. On our pre-patterned substrate (Fig. 1(b)), this favors positioning of the islands inside the holes.

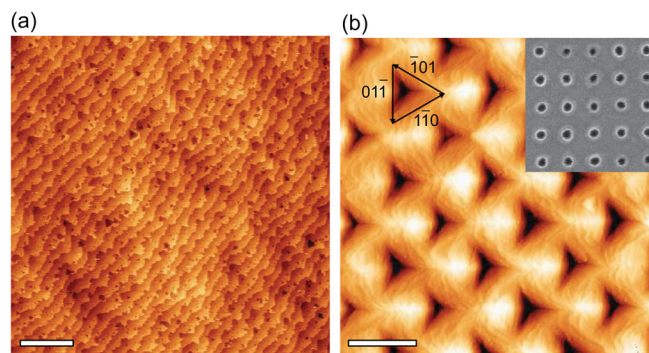


FIG. 1. (a) STM images of the Si(111) after wet cleaning and passivation out of the patterned area. Surface exhibits an array of steps due to the miscut of the substrate. Scale bar is 500 nm. (b) STM image of the patterned Si(111) exhibiting an array of triangular holes due to (111) planes revelation during NH_4F dipping. Steps are also visible and their density is much higher in the hole due to the local higher miscut angle. Scale bar is 80 nm. Inset is a SEM image of the hole array (periodicity 80 nm) prior to passivation and annealing under UHV.

To confirm this long range arrangement, Fourier transforms from large scale SEM images were taken inside and outside the patterned area. A cross section along the [1–10] axis, presented in Fig. 3(a), shows a series of peaks for the images taken in the patterned area (red curve). These peaks are representative of the periodicity of the island array (80 nm) and are not observed on images taken out of the patterned area (black curve). The fact that several orders of the periodicity peak are clearly observed comes from the long range order extending across all the SEM images taken in the patterned area. This is at variance with the situation outside the artificial hole array, where only short range order is observed with a central peak on the Fourier transform.

While the long range order is very good, small fluctuations in the island position inside a given hole are observed (see Fig. 2 and inset), so that the alignment is not perfectly straight at the nanometer scale. Looking at the patterned surface (Fig. 1(b)), the high curvature region around a hole covers a sizeable fraction of the array. Due to the fluctuations in the nucleation events, the growing nuclei are thus allowed to

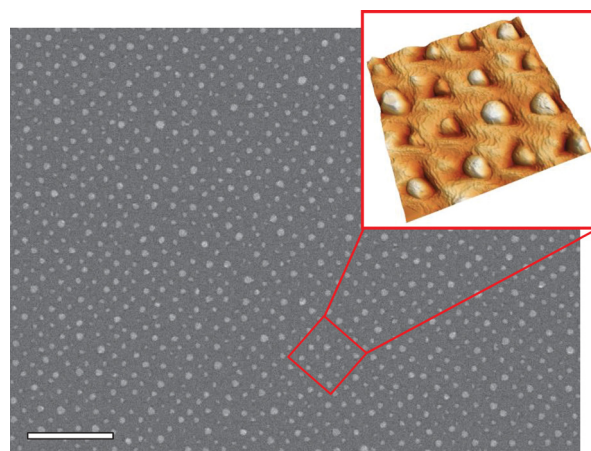


FIG. 2. SEM image of the self-organized growth of Au-Si islands on Si(111) surface patterned with an array of holes. Scale bar is 200 nm and distance between islands is 80 nm. Inset is a 3D STM image showing a regular arrangement of 4×4 islands.

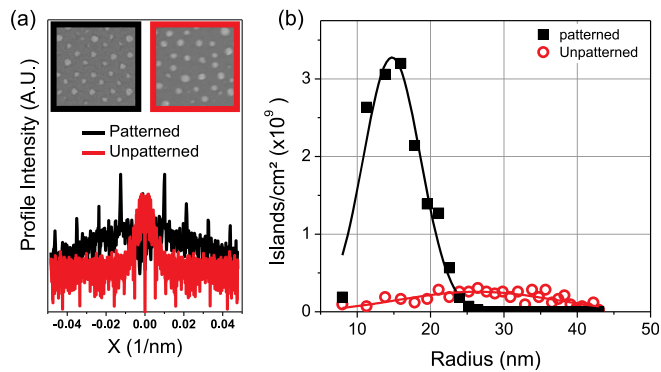


FIG. 3. (a) Profile intensity of the Fourier transform of SEM images taken in (left/black) and out (right/red) of the patterned area after Au growth. (b) Island size distribution taken in and out of the patterned area after Au growth. Squares and circles are experimental data whereas curves are Gaussian fits.

not be exactly at the same position in the holes, with variations on the 10 nm scale. This has the additional effect of widening the island size distribution compared to perfectly positioned islands as the capture area for each island is slightly different.²⁶ Nevertheless, the island size distribution is still found narrower in the patterned area than in the unpatterned one as shown in Fig. 3(b) where the distributions are displayed. Mean island radius and standard deviation are, respectively, 15 ± 4 nm and 26 ± 11 nm, from a fit of a Gaussian function to the experimental data. To further improve the growth template, a smaller pattern size/period ratio should give less fluctuation in island positions.

We studied the variation of the island density as a function of the growth temperature at fixed atomic flux, plotted in Figure 4. This analysis was performed on 2 kinds of substrates: (i) nominal Si(111) in areas without atomic steps obtained by electromigration-induced step bunching²⁷ and (ii) the patterned substrate previously described. Density measurements were performed on numerous large STM images and, concerning (ii), in the patterned area. In Fig. 4, the island density is normalized with respect to the hole

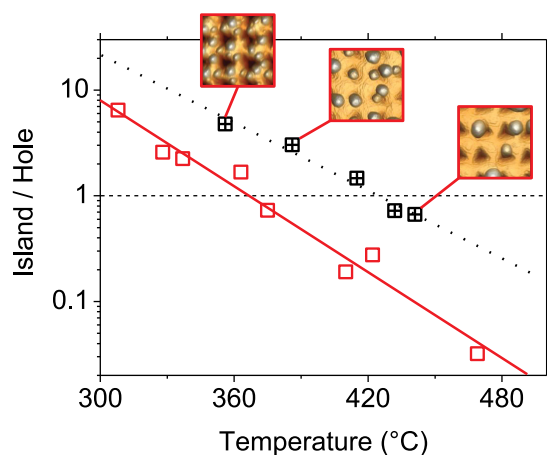


FIG. 4. Temperature dependence of the island density (normalized to the hole density) as a function of the growth temperature on two kinds of substrates: Red crossed squares correspond to 2D patterned substrate, black empty squares correspond to step-free substrate. Lines are guides for the eyes. Insets are typical STM images (240×240 nm²) at different growth temperatures.

density, so that 1 corresponds to 1 island per hole. A few typical images (240×240 nm²) are presented as insets in the case of (ii).

A general and expected decrease of the island density with increasing temperature is observed for both substrates. Indeed, increasing the growth temperature leads to a larger adatom diffusion length on the surface before nucleation, and thus to a larger distance between islands. On the patterned substrate, the density decreases from 5 to 0.8 islands per hole for growth temperatures between 355 °C and 440 °C. The island density is found systematically higher on the 2D patterned substrate than on the step-free substrate. The latter gives the diffusion length of Au adatoms on the Au-Si wetting layer, and this length appears reduced on the patterned surface. While at 360 °C the diffusion length on the Au-Si terraces should be enough to obtain 1 island per hole (Fig. 4, red line), 5 times more islands are seen on the patterned surface especially in between the holes (Fig. 4, black line and STM image). As seen in Fig. 1(b), the high density of steps due to the hole array extends beyond the holes themselves and is thus probably responsible for the diffusion length reduction as nucleation probability is increased at step edges. In the end the temperature had to be increased to 415 °C to obtain 1 island per hole. It should be pointed out that no plateau at this island density is observed on the temperature dependence above about 415 °C. Indeed at higher temperatures more and more holes are empty (Fig. 4), hinting at a disparity of island stability between neighboring holes so that the less stable disappear in favor of the most stable ones. Again this might be linked to a large pattern size/period ratio giving a dispersion in island positions inside the holes.

As a conclusion, we fabricated an array of metallic islands on silicon at the sub-100 nm scale by means of a self-organization process on pre-patterned substrates using e-beam lithography and etching. This approach allows to arbitrary tune the array pattern and density on mm² areas while preserving good crystalline quality of the nanometer-sized island.

¹H.-J. Freund, *Surf. Sci.* **500**, 271 (2002).

²X. D. Hoa, A. G. Kirk, and M. Tabrizian, *Biosens. Bioelectron.* **23**, 151 (2007).

³S. W. Boettcher, N. C. Strandwitz, M. Schierhorn, N. Lock, M. C. Lonergan, and G. D. Stucky, *Nature Mater.* **6**, 592 (2007).

⁴C. Y. Tsai, T. L. Chang, C. C. Chen, F. H. Ko, and P. H. Chen, *Microelectron. Eng.* **78–79**, 546 (2005).

⁵K. Westwater, D. P. Gosain, S. Tomiya, S. Usui, and H. Ruda, *J. Vac. Sci. Technol. B* **15**, 554 (1997).

⁶D. Takagi, Y. Homma, H. Hibino, S. Suzuki, and Y. Kobayashi, *Nano Lett.* **6**, 2642 (2006).

⁷A. Fleurence, G. Agnus, T. Maroutian, B. Bartenlian, P. Beauvillain, E. Moyaen, and M. Hanbueken, *Appl. Surf. Sci.* **254**, 3147 (2008).

⁸E. Moyaen, M. Macé, G. Agnus, A. Fleurence, T. Maroutian, F. Houzé, A. Stupakiewicz, L. Masson, B. Bartenlian, W. Wulfhekel, P. Beauvillain, and M. Hanbueken, *Appl. Phys. Lett.* **94**, 233101 (2009).

⁹K. V. Sarathlal, D. Kumar, and A. Gupta, *Appl. Phys. Lett.* **98**, 123111 (2011).

¹⁰T. W. H. Oates, A. Keller, S. Noda, and S. Facsko, *Appl. Phys. Lett.* **93**, 063106 (2008).

¹¹C. Lee and A.-L. Barabasi, *Appl. Phys. Lett.* **73**, 2651 (1998).

¹²H. Brune, M. Giovannini, K. Bromann, and K. Kern, *Nature* **394**, 451 (1998).

¹³V. Repain, J. M. Berroir, S. Rousset, and J. Lecoer, *Surf. Sci.* **447**, L152 (2000).

¹⁴B. Yang, F. Liu, and M. G. Lagally, *Phys. Rev. Lett.* **92**, 025502 (2004).

- ¹⁵Y.-J. Liu, Z.-Y. Zhang, Q. Zhao, and Y.-P. Zhao, *Appl. Phys. Lett.* **93**, 173106 (2008).
- ¹⁶T. Mårtensson, P. Carlberg, M. Borgstro, L. Montelius, W. Seifert, and L. Samuelson, *Nano Lett.* **4**, 699 (2004).
- ¹⁷Y. Homma, P. Finnie, T. Ogino, H. Noda, and T. Urisu, *J. Appl. Phys.* **86**, 3083 (1999); Y. Homma, P. Finnie, and T. Ogino, *Appl. Phys. Lett.* **74**, 815 (1999).
- ¹⁸T. Kitajima, B. Liu, and S. R. Leone, *Appl. Phys. Lett.* **80**, 497 (2002).
- ¹⁹Z. Zhong, P. Chen, Z. Jiang, and G. Bauer, *Appl. Phys. Lett.* **93**, 043106 (2008).
- ²⁰A. Rota, A. Martinez-Gil, G. Agnus, E. Moyon, T. Maroutian, B. Bartenlian, R. Mégy, M. Hanbücken, and P. Beauvillain, *Surf. Sci.* **600**, 1207 (2006).
- ²¹S. Y. Chou, P. R. Krauss, and P. J. Renstrom, *Science* **272**, 85 (1996).
- ²²G. S. Higashi, Y. J. Chabal, G. W. Trucks, and K. Raghavachari, *Appl. Phys. Lett.* **56**, 656 (1990).
- ²³P. Allongue, C. Henry de Villeneuve, S. Morin, R. Boukherroub, and D. D. M. Wayner, *Electrochim. Acta* **45**, 4591 (2000).
- ²⁴Y. J. Chabal, *Fundamental Aspects of Silicon Oxidation* (Springer, Berlin, 2001), pp.15–17.
- ²⁵B. Ressel, K. C. Prince, S. Heun, and Y. Homma, *J. Appl. Phys.* **93**, 3886 (2003).
- ²⁶P. A. Mulheran and J. A. Blackman, *Phys. Rev. B* **53**, 10261 (1996).
- ²⁷K. Yagi, H. Minoda, and M. Degawa, *Surf. Sci. Rep.* **43**, 45 (2001).